



## OPEN ACCESS

## EDITED BY

Stanislaw Mazur,  
Institute of Geological Sciences, Polish  
Academy of Sciences, Poland

## REVIEWED BY

Sreehari Lakshmanan,  
Shimane University, Japan  
Themiso O. Basupi,  
Botswana International University of  
Science and Technology, Botswana

## \*CORRESPONDENCE

Chih-Tung Chen,  
✉ [chitung@ncu.edu.tw](mailto:chitung@ncu.edu.tw),  
✉ [kthomasch@gmail.com](mailto:kthomasch@gmail.com)

RECEIVED 07 December 2022

ACCEPTED 18 April 2023

PUBLISHED 09 May 2023

## CITATION

Lo Y-C, Chen C-T, Lo C-H, Chung S-L  
and Yeh M-W (2023), Record of short-  
lived “orogen” on Eurasian continental  
margin by South China Sea obduction  
preserved in Taiwan collision.  
*Front. Earth Sci.* 11:1118520.  
doi: 10.3389/feart.2023.1118520

## COPYRIGHT

© 2023 Lo, Chen, Lo, Chung and Yeh.  
This is an open-access article distributed  
under the terms of the [Creative  
Commons Attribution License \(CC BY\)](https://creativecommons.org/licenses/by/4.0/).  
The use, distribution or reproduction in  
other forums is permitted, provided the  
original author(s) and the copyright  
owner(s) are credited and that the original  
publication in this journal is cited, in  
accordance with accepted academic  
practice. No use, distribution or  
reproduction is permitted which does not  
comply with these terms.

# Record of short-lived “orogen” on Eurasian continental margin by South China Sea obduction preserved in Taiwan collision

Yun-Chieh Lo<sup>1</sup>, Chih-Tung Chen<sup>2\*</sup>, Ching-Hua Lo<sup>1</sup>,  
Sun-Lin Chung<sup>1,3</sup> and Meng-Wan Yeh<sup>4</sup>

<sup>1</sup>Department of Geosciences, National Taiwan University, Taipei, Taiwan, <sup>2</sup>Department of Earth Sciences, National Central University, Taoyuan, Taiwan, <sup>3</sup>Institute of Earth Sciences, Academia Sinica, Taipei, Taiwan, <sup>4</sup>Department of Earth Sciences, National Taiwan Normal University, Taipei, Taiwan

The Taiwan mountain belt is the result of an arc-continent collision following the total subduction of the South China Sea and subsequent closure of the Luzon forearc, a process important in the accretionary growth of continents. Due to the oblique convergence, the southern tip of Taiwan Island is experiencing incipient collision, which is key to observing the oceanic-continent subduction transition. Within the monotonous turbidite extensively exposed on the Hengchun Peninsula as an uplifted Manila Trench accretionary wedge, the Shihmen Conglomerate, as a few intercalated lenses of coarse mafic pebbles, represents a dramatic change in sediment provenance and the causal tectonic event. New zircon U-Pb and amphibole <sup>40</sup>Ar/<sup>39</sup>Ar ages are obtained from sediments, including sands and mafic pebbles that are either gabbro or foliated amphibolite. The 22–24 Ma zircon crystallization ages confirm the South China Sea origin of the mafic clasts, while the much younger  $13 \pm 2$  Ma amphibole <sup>40</sup>Ar/<sup>39</sup>Ar isochron ages from foliated amphibolites suggest a later thermal-tectonic event other than seafloor metamorphism. The amphibole <sup>40</sup>Ar/<sup>39</sup>Ar ages overlap with the biostratigraphic age (~11–14 Ma), indicating that the mafic source rocks were exhumed and eroded in a high-relief topography immediately after metamorphism. Detrital zircon U-Pb ages from a sandy layer within the conglomerate are also mostly identical to those from the mafic pebbles. Since the paleocurrent of the Shihmen Conglomerate was similar to that of the neighboring turbidites, which were derived from major rivers draining the southeastern Chinese continent, the provenance of the mafic pebbles and sands was best explained as an isolated subaerial mountain on the Eurasian continental margin with a very limited temporal and spatial extent, as the detrital products are poorly distributed. The most likely cause of the ephemeral mountain was the obduction of the South China Sea onto the Eurasian continental margin when the latter first impinged on the Philippine Sea Plate at the Manila Trench, where the gabbroic oceanic crust was uplifted and exhumed, followed by dynamic metamorphism along the basal thrust.

## KEYWORDS

Eurasian continental margin, South China Sea, Taiwan mountain belt, ophiolite obduction, zircon U-Pb dating, <sup>40</sup>Ar/<sup>39</sup>Ar dating

# 1 Introduction

Arc-continent collisions are an integral part of the accretionary growth of continents (Sengor et al., 1993; Jahn et al., 2000) and have crucial and varying effects on the tectonic evolution of continental margins (Ryan and Dewey, 2019). One of the key questions is how an initially subducted continental margin can affect the state and configuration of the subduction zone and the overall convergent plate boundary, as increased roughness of the subduction interface is known to heighten the friction of the subduction megathrust (Lallemand et al., 2018; Tan et al., 2022). Coupling changes along the subduction interface may propagate laterally or across the ocean basin to influence continent-ocean transition (COT) tectonics, including faulting and ophiolite obduction (Searle et al., 2022). Within the complex geodynamics of the Indo-Pacific and eastern Eurasia region, the active Taiwan mountain belt serves as a natural laboratory for studying arc-continent collision processes (Byrne et al., 2011) under a well-defined tectonic framework (Figure 1, inset) that allows synchronous observation of orogenesis from initiation in the south to the final stage in the north due to oblique convergence (Suppe, 1988). Near the southern end of the island, the uplifted accretionary wedge as the Hengchun Peninsula sits on the transition from oceanic subduction to collision (Shyu et al., 2005; Figure 1); the tectonic regime change is documented in local geological structures (Chang et al., 2003) and may also be reflected in sedimentological variations within the off-scraped South China Sea marine sequence. One such anomaly is the occurrence of

puzzling conglomerates composed almost exclusively of coarse mafic pebbles (Chen et al., 1985; Sung, 1991), indicating the presence of former ophiolitic mountain ranges in the periphery of the South China Sea (Pelletier and Stephan, 1986). How such a transient “mountain building” event was generated would shed light on the impact of continental subduction on the subduction zone dynamics and tectonic evolution of the COT and is therefore worthy of detailed investigation.

The Taiwan mountain belt is the result of active oblique convergence between the Eurasian and Philippine Sea plates (Suppe, 1988; Teng, 1990) and began with subduction of the Eurasian continental margin along the Manila Trench followed by the collision of the Luzon Arc (Malavielle et al., 2002) (Figure 1, inset). Prior to the orogeny at ~15 Ma (evidenced by the onset of Luzon Arc volcanism; Song and Lo, 2002; Lai et al., 2018), the Manila Trench began to receive the South China Sea, which was formed along slowly spreading ridges (Chung and Sun, 1992) from ~37 to 15 Ma (Briais et al., 1993; Yeh et al., 2010). The Hengchun Ridge formed above the trench is an accretionary prism composed of the fault-folded South China Sea marine sequence and becomes larger and subaerial as the Hengchun Peninsula in the north, where the South China Sea is completely consumed and the continental margin enters the subduction zone. The exposed Late Miocene pelagic turbidite sequence accreted to the accretionary wedge is collectively termed the Mutan Formation, and lenses of meta-mafic conglomerates are found intercalated in its lower part and called the Shihmen Conglomerate (Chen et al., 1985; Figure 1).

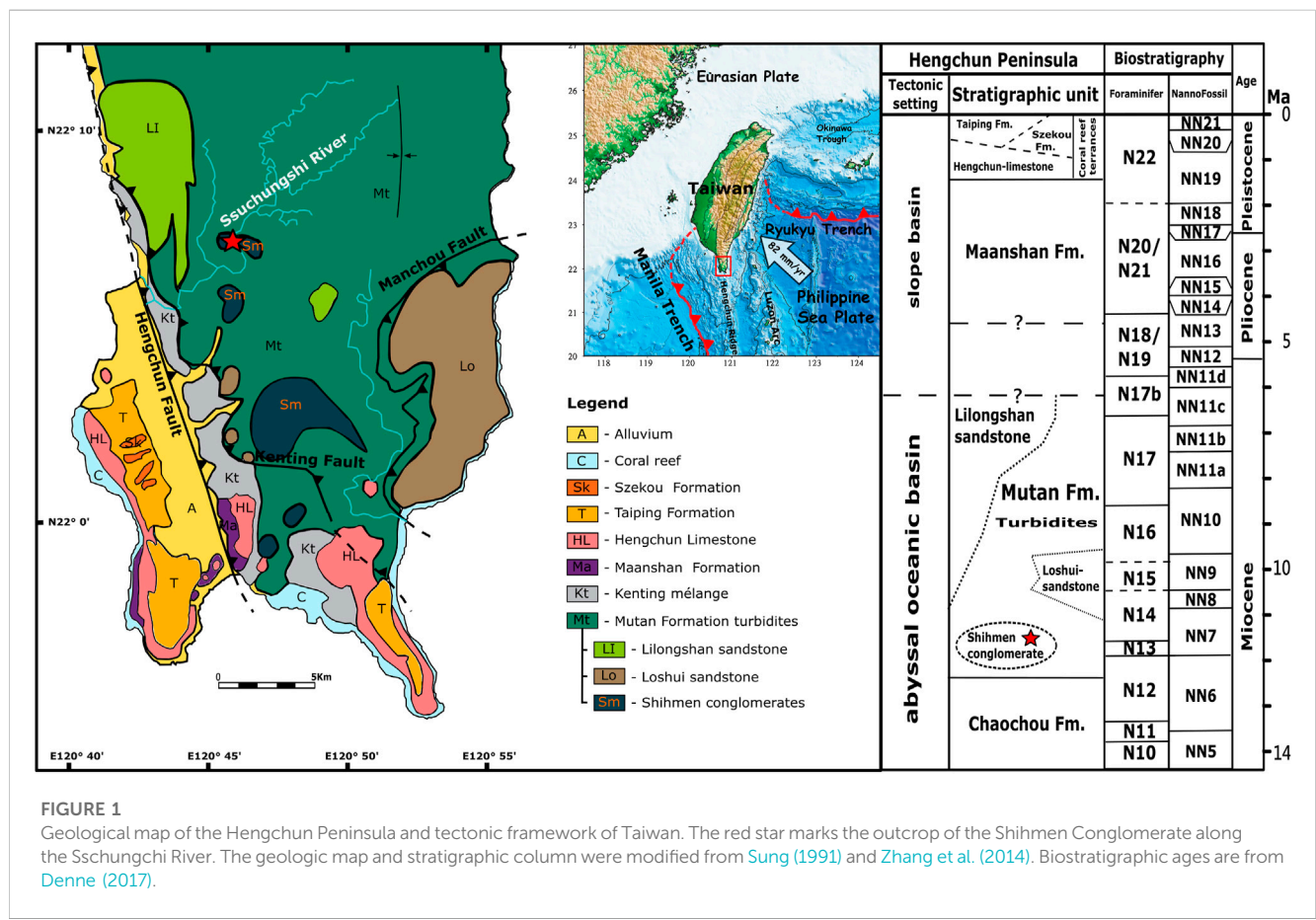


**FIGURE 1** Geological map of the Hengchun Peninsula and tectonic framework of Taiwan. The red star marks the outcrop of the Shihmen Conglomerate along the Ss chung chi River. The geologic map and stratigraphic column were modified from Sung (1991) and Zhang et al. (2014). Biostratigraphic ages are from Denne (2017).

How these rounded and well-sorted, sometimes intensely foliated mafic pebbles were generated and deposited in the deep basin of the northern South China Sea has intrigued researchers with hypotheses including an emergent oceanic crust (Page and Lan, 1983; Zhang et al., 2022), a reworking of obducted ophiolites (Pelletier and Stephan, 1986), temporary uplift and collapse of seamounts (Tian et al., 2019) or eastward deep-water transport (Cui et al., 2021; Meng et al., 2021). A crucial missing key to resolving the provenance and tectonic origin of the Shihmen Conglomerate lies in exact chronological constraints on the formation and metamorphism of the gabbroic protolith and is addressed here by applying zircon U-Pb dating analysis for both pebbles and matrix sands and amphibole  $^{40}\text{Ar}/^{39}\text{Ar}$  dating analysis for foliated amphibolitic meta-gabbro pebbles. The acquired ages are incorporated into the local stratigraphic and tectonic framework, suggesting a temporary fringe mini-orogen resulting from the South China Sea obduction onto the Eurasian continental margin in response to the incipient collision of the Manila subduction system to the north, where the Taiwan orogen initially began.

## 2 Geologic setting and sample description

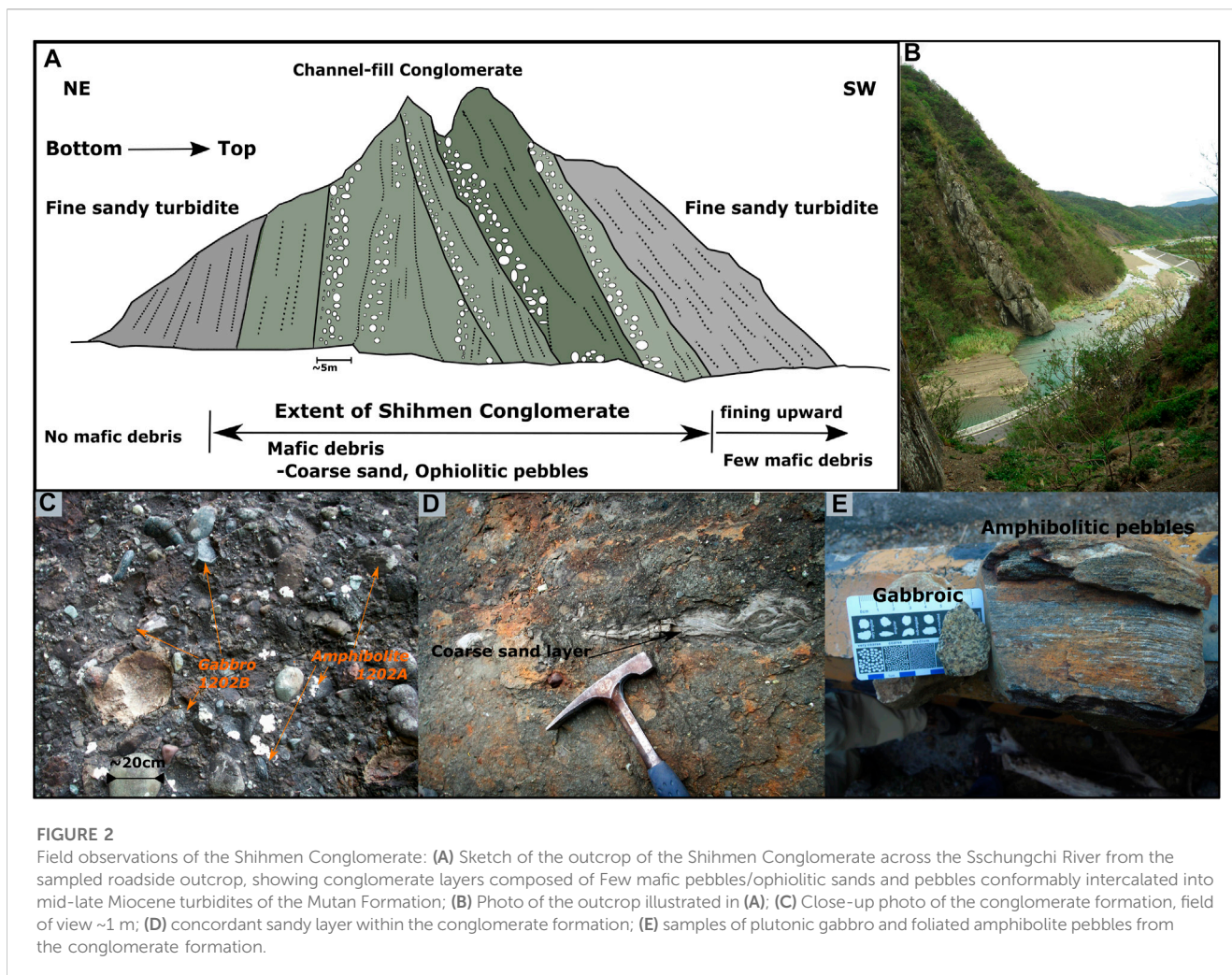
The Hengchun Peninsula at the southernmost tip of Taiwan Island represents the youngest segment of the orogenic system due to the oblique plate convergence (Suppe, 1988; Shyu et al., 2005; Figure 1, inset). Fault-folded Late-Miocene turbidites of the Mutan Formation with N-S structural grains (Sung, 1991; Chang et al., 2003; 2009a) comprise the main hilly terrane of the peninsula as a southern extension of the Backbone Range, and are bounded to the west and southwest by the Kenting mélangé, a paleo-subduction channel relict of the Manila Trench (Lu and Hsu, 1992; Chang et al., 2003; Figure 1). Both the Mutan Formation and the Kenting mélangé outcrop east of the active sinistral-reversal Hengchun Fault; the small plain of the Hengchun Basin in the immediate footwall and the uplifted West Hengchun Tableland of Quaternary limestone reefs further west make up the rest of the peninsula (Figure 1), demonstrating westward propagation of the trench/deformation front and widening and thickening of the accretionary wedge (Chang et al., 2003; Lin et al., 2009). To the north, further exhumation leads to exposure of the slate Lushan Formation, the low-grade metamorphosed pelagic South China Sea deposits, in the Backbone Range (Chen et al., 1983; Beysac et al., 2007).

The Mutan Formation is composed of deep-sea fan turbidite sequences with shale-sandstone alternations (Hu and Tsan, 1984; Figure 1) of planktic foraminiferal biozones N14–17 (Chang, 1964) and southeastern mainland China continent provenance as indicated by sandstone lithology, paleocurrent, and detrital zircon dating data (Pelletier and Stephan, 1986; Chang et al., 2003; Zhang et al., 2014; Tsai et al., 2020). Several lenticular bodies of coarser deposits, including the Shihmen Conglomerate, Lilongshan Sandstone, Shihzutou Sandstone, and Loshui Sandstone, are intercalated within the Mutan turbidite as products of major submarine channels draining from the slope of the Chinese continental margin (Pelletier and Stephan, 1986; Sung, 1991;

Chang et al., 2003). While the Mutan turbidite and the other lenticular units are of continental provenance, the Shihmen Conglomerate stands out with dominant rounded mafic clasts including gabbro, basalt and diabase, and foliated amphibolite, supplemented by minor granitic gneiss, siliceous schist, quartz vein and marble/limestone, representing erosional products of emergent oceanic crust (Page and Lan, 1983). The age of deposition of the Shihmen Conglomerate has been constrained at ~11–14 Ma from biostratigraphic records (NN6; Chi, 1982; ~N14; Sung, 1991). Previous attempts to date mafic pebbles from the Ss chungshi Gorge outcrop of the Shihmen Conglomerate have all yielded early Miocene results, including K-Ar dating of amphibolite amphiboles (22–23 Ma, Pelletier and Stephan, 1986) and zircons from both gabbro ( $23.78 \pm 0.41$ , Meng et al., 2021;  $23.73 \pm 0.69$  Ma; Cui et al., 2021) and amphibolite ( $24.2 \pm 1.1$  Ma, Tian et al., 2019) pebbles, within the age range of the South China Sea spreading. Therefore, the Shihmen Conglomerate signified a dramatic change in the provenance environment along the Eurasian continental margin, such as an obduction event (Pelletier and Stephan, 1986), while others speculated that the site of obduction was the accretionary wedge (Page and Lan, 1983) or rifted continental sliver (Suppe, 1988) along the southeastern side of the South China Sea.

The most accessible outcrop of the Shihmen conglomerate is along the Ss chungchi River at the ancient Shihmen (“Rock Gate”) battlefield. The sampled roadside outcrop (E 120.76118, N 22.11190) is about 40 m wide and ~100 m high, exposing sub-vertical conglomerate beds that trend NW-SE and dip steeply to the west, consistent with the neighboring Mutan turbidite (Figures 2A,B). The conglomerate content is dominated by rounded and sub-rounded pebbles of gabbro and foliated amphibolite and minor siliceous and chloritic schist and quartz vein; pebble diameters vary from 1 to 15 cm and sometimes reach ~30 cm (Figure 2C). Coarse sands make up the matrix in addition to occasional concordant sandstone beds (Figure 2D). To unravel the tectonic characteristics of the provenance, foliated amphibolite pebbles, plutonic gabbro pebbles, and sands from the intercalated sandy layer (Figures 2C–E) were sampled for zircon U-Pb and amphibole  $^{40}\text{Ar}/^{39}\text{Ar}$  dating analyses. The ages obtained were then correlated with regional seafloor spreading and plate convergence histories for a comprehensive geodynamic interpretation.

Sample 1202A is a collection of more than 5 kg of fresh, sub-rounded, foliated amphibolite pebbles 10–20 cm in diameter collected from the conglomerate outcrop. The sampled pebbles exhibit strong penetrating amphibolitic foliation with mm-thick repeating amphibole and plagioclase bands throughout or in part of the pebbles (Figure 2E). Under the microscope, the cleavage domain is mainly composed of smaller (lengths less than 300  $\mu\text{m}$ ) aligned amphibole grains with minor opaques, and the adjacent plagioclase layers are of larger grain size (up to 0.5 mm in diameter) with twinning and interlobular boundaries (Figure 3A). Ductile shear deformation during recrystallization is evident in the metamorphic paragenesis of lined amphiboles and the interlobate recrystallizing (grain boundary migration) plagioclase grains (Figure 3A) and may have persisted into post-recrystallization brittle-ductile states as evidenced by albite twinning in plagioclase (Figure 3A). The protolith of the



foliated amphibolites is probably gabbro, as some of the pebbles preserve relict pyroxene (Figure 3A) and display plutonic texture where not foliated, as indicated by geochemical analyses (Page and Lan, 1983; Pelletier and Stephan, 1986). Both zircon and amphibole are separated for dating analyses.

Sample 1202B is a collection of more than 5 kg of fresh, sub-rounded gabbro pebbles, 10–20 cm in length, collected from the conglomerate outcrop (Figure 2C). The pebbles exhibit a phaneritic plutonic texture with interlocking euhedral tabular plagioclase crystals and mostly anhedral pyroxene grains (Figure 3B). Some of the pyroxene grains have been substituted by amphibole, but the replacement is rather minor and does not yield sufficient amphibole grains for  $^{40}\text{Ar}/^{39}\text{Ar}$  dating analysis. Zircon is extracted for U-Pb dating to determine the crystallization age of the gabbro, which indicates the timing of ocean crust formation.

Sample 1202C is a sandstone sample from a ~20 cm-thick concordant sandy layer within the conglomerate (Figure 2). The medium-coarse sandy layer is monotonous without pebbles or grading texture and consists of 0.1–1 mm rounded grains of mostly greenish mafic clasts (Figure 3C). Zircon is separated for U-Pb ages to resolve the provenance of the sandy deposits.

## 3 Geochronological analyses

### 3.1 U-Pb dating

Zircons from each sample were separated using conventional magnetic and heavy-liquid methods. After separation, zircon grains with crystal lengths >60–200  $\mu\text{m}$  were linearly mounted with epoxy resin and then polished to expose the interior grains for U-Pb dating. Prior to U-Pb analysis, cathodoluminescence (CL) images were taken at the Institute of Earth Sciences, Academia Sinica, Taiwan. CL pictures help to locate analytical spots by examining the internal structures of individual zircon grains and avoiding inclusions during analysis. *In-situ* laser ablation inductively coupled plasma mass spectrometry (LA-ICP-MS) U-Pb dating was performed using an Agilent 7500s quadrupole ICP-MS coupled with a 193 nm Analyte G2 excimer laser ablation system housed at the Department of Geosciences, National Taiwan University. The beam size of the laser ablation pits is ~30  $\mu\text{m}$  in diameter. Measured U-Th-Pb isotope ratios were calculated using the GLITTER 4.4 (GEMOC) software, and calibration was performed using the zircon standard GJ-1 aged at  $608.5 \pm 0.4$  Ma (Jackson et al., 2004). Zircon 91,500 ( $1065 \pm$

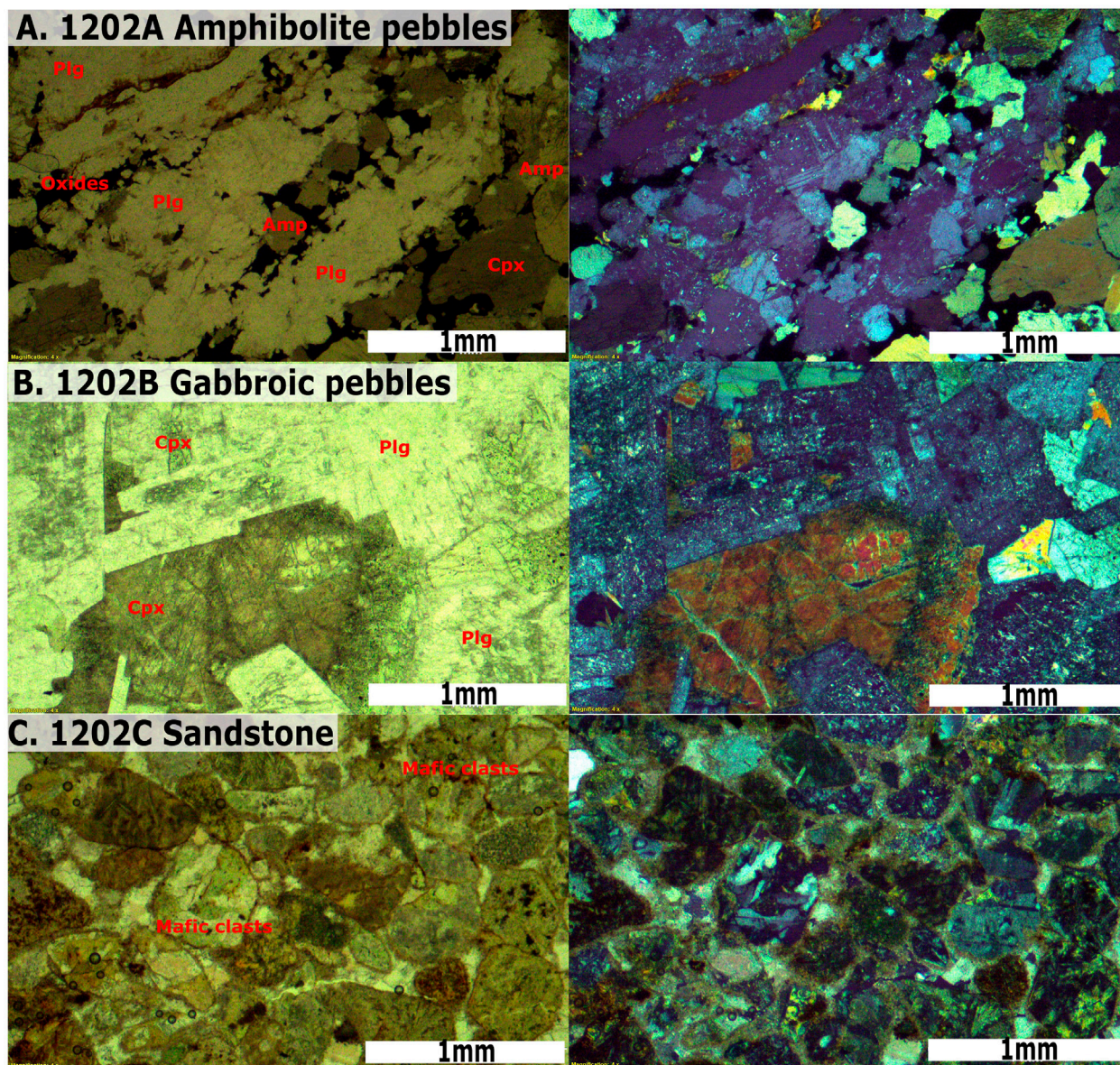


FIGURE 3

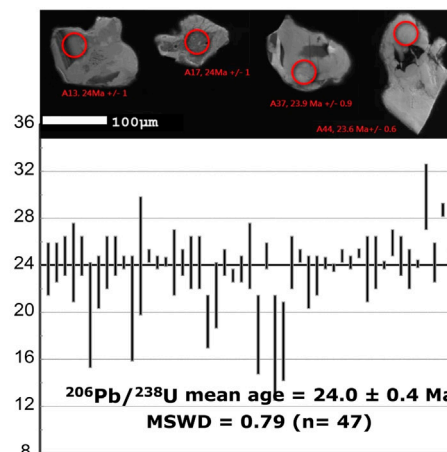
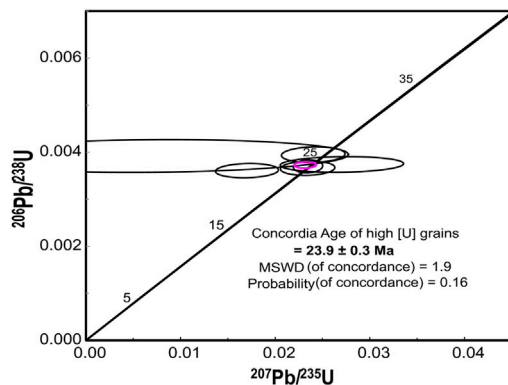
Photomicrographs of the analyzed samples (planar and cross-polarized light for the left and right, respectively): (A) Foliated amphibolite pebbles (sample 1202A); (B) Gabbroic pebbles (sample 1202B); (C) Sandstone (sample 1202C) from a concordant sandy layer within the conglomerate composed of coarse sub-rounded mafic clasts. The white scale bar is 1 mm in length. Plg: plagioclase; Amp: amphibole; Cpx: clinopyroxene; Qtz: quartz.

0.4 Ma; Wiedenbeck et al., 1995) and Plešovice ( $337.1 \pm 0.4$  Ma; Sláma et al., 2008) were analyzed as secondary standards for data quality control in each analysis cycle. Operating conditions and analytical procedures followed (Chiu et al. 2009). Common lead in zircons was corrected with the lead correction function proposed by Andersen (2002), and weighted mean U-Pb ages and Concordia plots were then conducted using Isoplot 4.15. (Ludwig, 2008). For U-Pb ages <50 Ma,  $^{206}\text{Pb}/^{238}\text{U}$  ages are chosen without consideration of concordance due to the low U concentration of mafic samples and the imprecision of  $^{207}\text{Pb}$  measurements for such young zircons using the LA-ICPMS method (Gehrels et al., 2008; Spencer et al., 2016).

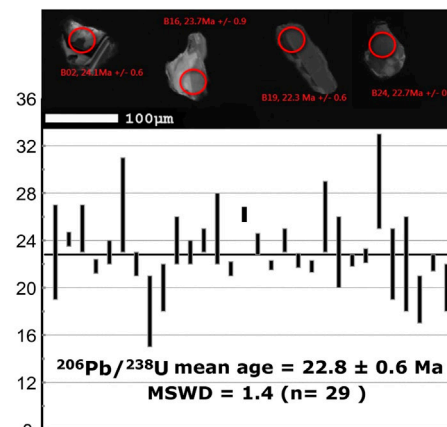
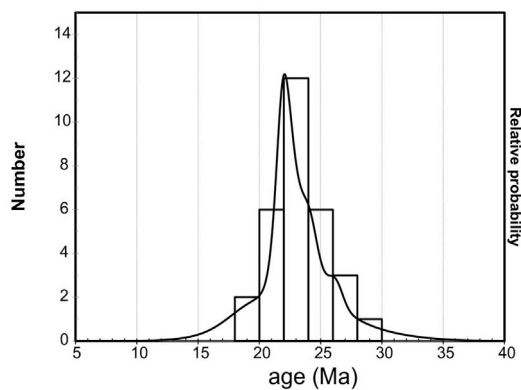
### 3.2 $^{40}\text{Ar}/^{39}\text{Ar}$ dating

For  $^{40}\text{Ar}/^{39}\text{Ar}$  dating, samples and standards were cleaned with an ultrasonic bath in acetone, alcohol, and deionized water, respectively, and then dried. Approximately 250 mg of amphibole separated from amphibolite pebbles was packaged and irradiated along with standards in the VT-C position of the Tsing-Hua Open-Pool Reactor (THOR) at Tsing-Hua University, Taiwan. Fish Canyon Sanidine (FCs) standard of  $28.10 \pm 0.04$  Ma (Spell and McDougall, 2003) was used to monitor the neutron flux, and the J-value of  $0.0047937 \pm 0.000025$  at the 1-sigma level was obtained from the analyses of FCs adjacent to the sample.

**A 1202A amphibolite pebbles**



**B 1202B gabbro pebbles**



**C 1202C sandstone**

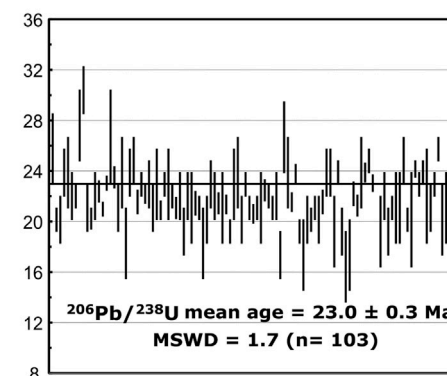
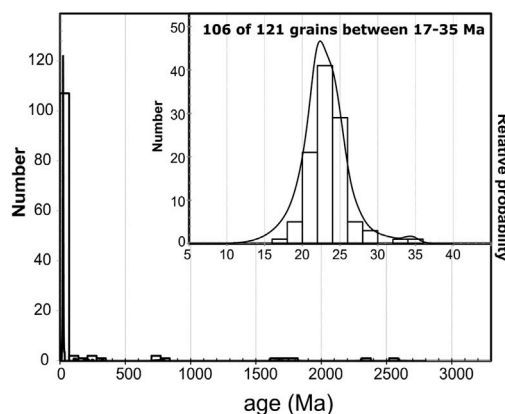


**FIGURE 4**

Zircon U-Pb dating results: (A) Sample 1202A of amphibolite pebbles yields a weighted mean age of  $24.0 \pm 0.4$  Ma, shown in the red circle; (B)  $^{206}\text{Pb}/^{238}\text{U}$  ages of sample 1202B of gabbroic pebbles fall between 18 and 29 Ma with a weighted mean age of  $22.8 \pm 0.6$  Ma; (C) 88% of the detrital zircons in the concordant sandy layer of sample 1202C show  $^{206}\text{Pb}/^{238}\text{U}$  ages of 17–35 Ma with a weighted mean of  $23.0 \pm 0.3$  Ma.

The sample was loaded (without any other sample or standard) into an ultra-high vacuum laser chamber and baked at  $150^\circ\text{C}$  for over 24 h to remove atmospheric contamination prior to analysis.

Argon was extracted using the single-grain total fusion method with a Synrad 48-1  $\text{CO}_2$  laser fusion system attached to a VG3600 mass spectrometer at National Taiwan Normal

University (NTNU). Before isotopic analysis, the sample gas was purified by a Ti-sponge for 3 min and then by two getters (one kept at 450 C and the other at room temperature) for 5 min to remove active gases (e.g., CO<sub>2</sub>, H<sub>2</sub>O, CH<sub>4</sub>). Detailed instrumental and analytical procedures are outlined in Lo et al. (2002). Data processing, including peak intensity regression and corrections for blanks, mass spectrometer discrimination, isotopic decay, and neutron-induced interference reactions, was performed using the ArArCALC software of Koppers (2002). The atmospheric argon ratio of 298.56 ± 0.31 was suggested by Lee et al. (2006). Isochron and weighted mean age re-statistics were obtained using IsoplotR (Vermeesch, 2018). Uncertainties in ages were reported as one standard deviation, taking into account errors in J-values, standard mineral ages, and isotopic interference factors.

### 3.3 Dating results

#### 3.3.1 U-Pb zircon geochronology

Zircons from the foliated amphibolite pebbles (1202A) appeared as transparent and colorless, occurring as truncated to prismatic crystals with sharp facets and some rounded terminations. Grain lengths ranged from ~100 to 300 μm with aspect ratios ranging from 1:1 to 3:1. A total of 51 zircon grains were analyzed and the U-Pb age results were concentrated in the 21–25 Ma interval, yielding a weighted mean age of 24.0 ± 0.4 Ma (MSWD = 0.79, n = 47), with high U-content grains that could have a Concordia age of 23.9 ± 0.3 Ma (MSWD = 1.9) (Figure 4A, and Supplementary Table S1 for detailed data). Most zircon crystals showed oscillatory zoning, but only one large zircon grain was found possessing a 34 Ma inherited core and a 23.8 Ma rim overgrowth; no other inherited cores or visible rim growth were found. Uranium concentrations in the zircons range from 20 to 1847 ppm, with most grains <200 ppm. The younger cluster had a lower U content and higher age uncertainty. All analyses yielded Th/U values >0.1 (0.19–1.38) implying a magmatic origin for all dated zircons (Williams and Claesson, 1987; Vavra et al., 1996; Hoskin and Black, 2000; Hartmann and Santos, 2004).

Zircons from gabbroic pebbles (1202B) appeared as euhedral to subhedral, generally colorless and transparent, and equivalent to long columnar grains with lengths of ~80–200 μm and aspect ratios ranging from 4:1 to 1:1. All U-Pb dating results fall between 18 and 29 Ma with a single major peak and a weighted mean age of 22.8 ± 0.6 Ma (MSWD = 1.4) (Figure 4B; Supplementary Table S2). The wide range of U contents (30–1942 ppm) with all Th/U values >0.1 (0.16–1.61) also suggested a magmatic origin of zircon crystallization.

A total of 121 zircon grains, ranging in length from ~50 to 250 μm, were recovered from the sandstone (1202C). Most of the U-Pb dating results fell in the 17–34.5 Ma age range (106 of 121, 88%) with a weighted mean age of 23.0 ± 0.3 Ma (MSWD = 1.7, n = 103), and the remainder had ages ranging from 100 to 2600 Ma (14 of 121, 12%) (Figure 4C; Supplementary Table S3). Most grains yielded ages in the 17–34.5 Ma age range and exhibited low uranium contents of <150 ppm, with Th/U values >0.1 (0.05–1.89, only 2 grains <0.1).

#### 3.3.2 <sup>40</sup>Ar/<sup>39</sup>Ar amphibole geochronology

Amphiboles from the foliated amphibolite pebbles (1202A) yielded apparent <sup>40</sup>Ar/<sup>39</sup>Ar ages between 10.8 and 24.3 Ma with a weighted mean age of 14.9 ± 0.7 Ma for the main cluster (Figure 5B; Supplementary Table S4), while the uncertainty for individual analyses was high, up to ~20%, due to the low K content and high Ca/K ratios. Excess argon was found in a few analyses of apparent ~24 Ma results, so the inverse isochron age of 13.3 ± 2.0 Ma with a <sup>40</sup>Ar/<sup>36</sup>Ar intercept of 302.0 ± 4.1 from the younger main cluster was preferred (Figure 5B).

## 4 Discussion

### 4.1 Provenance of sediments

To determine how the ophiolite-dominated Shihmen Conglomerate was intercalated with pelagic turbidites from the South China Sea, the provenance properties of the pebbles have to be investigated. The data reported here can elucidate key provenance characteristics of the pebbles, such as the parent rock affinities, formation ages, and thermal-metamorphic history for amphibolitic clasts. Both plutonic gabbro and foliated amphibolite pebbles yielded similar U-Pb zircon crystallization ages of 22–24 Ma (Figures 4A,B), indicating that the dated gabbro was the protolith of the foliated amphibolites. The age results are consistent with geochemical analyses indicating a common ocean ridge tholeiite origin for both the gabbroic and amphibolite clasts (Page and Lan, 1983; Pelletier and Stephan, 1986). The gabbro crystallization age is similar to that reported by Wang et al. (2012) and falls within the time span of South China Sea spreading (~37–~15 Ma; Taylor and Hayes, 1983; Briais et al., 1993; Yeh et al., 2010), therefore the South China Sea crust should be the common source of these mafic materials since the oceanic crust of the westernmost Philippine Sea plate has been interpreted as either Eocene (~50–~40 Ma; Karig et al., 1975; Sibuet et al., 2002) or Cretaceous (~130–~120 Ma; Deschamps et al., 2000; Queano et al., 2007), ruling out the upper Manila Trench plate as a possible source. The dating results are also consistent with previous attempts to analyze these mafic pebbles (Pelletier and Stephan, 1986; Tian et al., 2019; Cui et al., 2021; Meng et al., 2021), and they also concur with the paleocurrent analyses pointing to Eurasian-side sources instead of the overriding plate (Chang et al., 2003).

### 4.2 Metamorphism of the amphibolite pebbles

The cause of metamorphism on the foliated amphibolite could be inferred from the <sup>40</sup>Ar/<sup>39</sup>Ar amphibole ages. Since the turbidite sequence exposed on the Hengchun Peninsula is not metamorphosed with a maximum peak temperature <200°C as suggested by vitrinite reflectance constraints (Zhang et al., 2016), the K-Ar isotope system of amphibole, with much higher closure temperatures (~490–578°C, Harrison, 1982), must have remained closed during subduction to accretionary wedge stages. The obtained isochron age of 13.3 ± 2.0 Ma, roughly 10 million years younger than the gabbro crystallization age from zircon U-Pb dating, also rules out

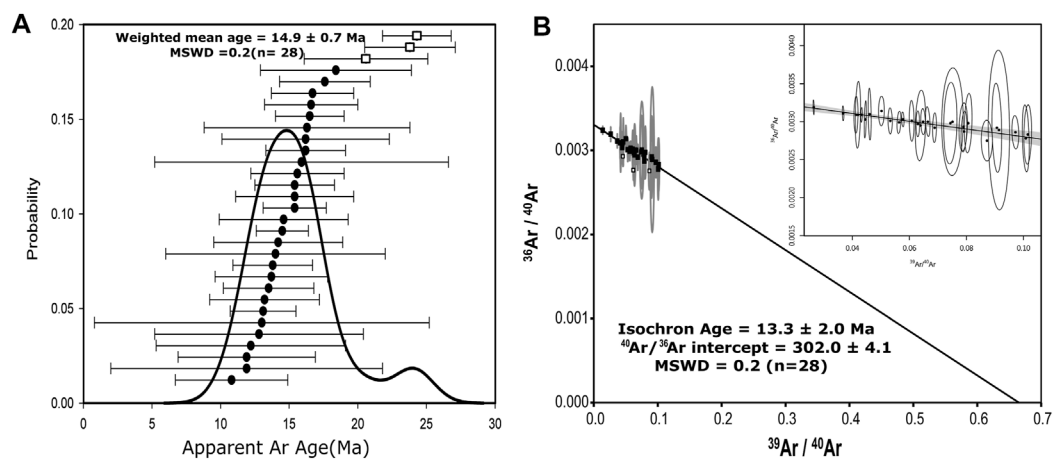


FIGURE 5

Results of laser-fusion  $^{40}\text{Ar}/^{39}\text{Ar}$  dating for amphibole from sample 1202A foliated amphibolite pebbles: (A) Distribution of apparent ages showing a main cluster (excluding those in the square) with a weighted mean age of  $14.9 \pm 0.7$  Ma; (B) inverse isochron plot yielding a  $^{40}\text{Ar}/^{39}\text{Ar}$  intercept age of  $13.3 \pm 2.0$  Ma with a  $^{40}\text{Ar}/^{36}\text{Ar}$  initial value of  $302.0 \pm 4.1$  for the main cluster. The inset displays the data distribution in detail.

sub-seafloor metamorphism as the main source, which typically occurs immediately after oceanic lithosphere formation along mid-ocean ridges with proximal heating and generally produces extensive veining and sulfide deposits indicative of intense fluid-rock interactions (Frost and Frost, 2014). The foliated amphibolite pebbles are mostly vein-free and exhibit significant ductile shearing as the aligned amphibole crystals and dynamically recrystallizing albite grains (Figures 3A,B), which is characteristic of tectonic deformation along the major shear zone rather than metasomatic seafloor metamorphism. The  $^{40}\text{Ar}/^{39}\text{Ar}$  amphibole ages record either amphibole paragenesis of both metamorphism and shearing or cooling during the subsequent exhumation. These would indicate that part of the 22–24 Ma gabbroic oceanic crust that is the source of the Shihmen Conglomerate must have been dynamically metamorphosed at  $\sim 13$  Ma or slightly earlier.

### 4.3 Tectonic implications

The occurrence of both gabbro and foliated amphibolite as rounded pebbles up to boulder sizes, together with other mafic clasts, indicates that a portion of the South China Sea crust was not only subaerial but must have possessed high relief to generate the torrential dumping of these coarse deposits into the South China Sea basin (Pelletier and Stephan, 1986). Detrital zircon U-Pb ages from the concordant sandy interlayer ( $23.0 \pm 0.3$  Ma, Figure 4C) are almost identical to those from the gabbroic ( $22.8 \pm 0.6$  Ma, Figure 4B) and foliated amphibolite pebbles ( $24.0 \pm 0.4$  Ma, Figure 4A), demonstrating that this ophiolitic source of the South China Sea ages produced both coarse pebbles and sands. The mafic magmatic origin of the dated zircon crystals from both pebbles and sandstones is also indicated by the low U content, which is mostly less than 100 ppm or even less than 10 ppm. The age spectrum of the Shihmen sands contrasts dramatically with normal sandstones of the Mutan Formation (Figure 6A) which are dominated by various pre-Cenozoic zircon

populations of the southeastern Chinese continent, including Yenshanian (200–65 Ma), Indosinian (250–200 Ma) and Luliangian (1900–1700 Ma) ages, with extremely rare Tertiary (<50 Ma) results (Zhang et al., 2014; Tsai et al., 2020). The turbidite layers adjacent to or in the periphery of the Shihmen deep-sea fan yield zircon populations (Figure 6B; Tsai et al., 2020; Meng et al., 2021) as diluted mixtures between Shihmen sands (Figure 6C) and normal Mutan sands (Figure 6A). Taking into account the inference from paleocurrent analyses that the sediment transport and source directions for the entire Mutan Formation were from the southeastern Chinese continent (Chang et al., 2003), the provenance of the Shihmen Conglomerate would be an ephemeral isolated rugged mountain composed exclusively of South China Sea ophiolite on the Eurasian continental margin, and the sediment routing system would be separated from the major rivers and their offshore extensions that drained the other common Mutan turbidites (Figure 7B). The tentatively postulated short-lived mountain building was most likely an obduction of the South China Sea crust onto the Eurasian continental margin at  $\sim 13$  Ma (Figure 7B); the lower-crustal gabbroic rocks along and near the basal thrust were dynamically recrystallized to foliated amphibolite in a metamorphic sole-like fashion (Searle et al., 2022; profile B-2 in Figure 7B) in the hanging-wall; both the upthrust gabbro and amphibolite, with minor other mafic lithologies, created a high-relief topography and delivered coarse detritus eastward to form deep-sea channel and fan turbidite deposits that are intercalated with normal Mutan sediments during the mid-Miocene at  $\sim 11$ – $13$  Ma (Sung, 1991, profile B-2 in Figure 7B). Another possibility is that the amphibolite was generated during subduction metamorphism of the South China Sea slab, and a portion of it was extruded back into the shallow crust and amalgamated with the obducting ophiolite sequence. The predominance of gabbroic lithologies in the pebbles may be due to the slow-spreading nature of the South China Sea crust (Chung and Sun, 1992; Briaies et al., 1993).

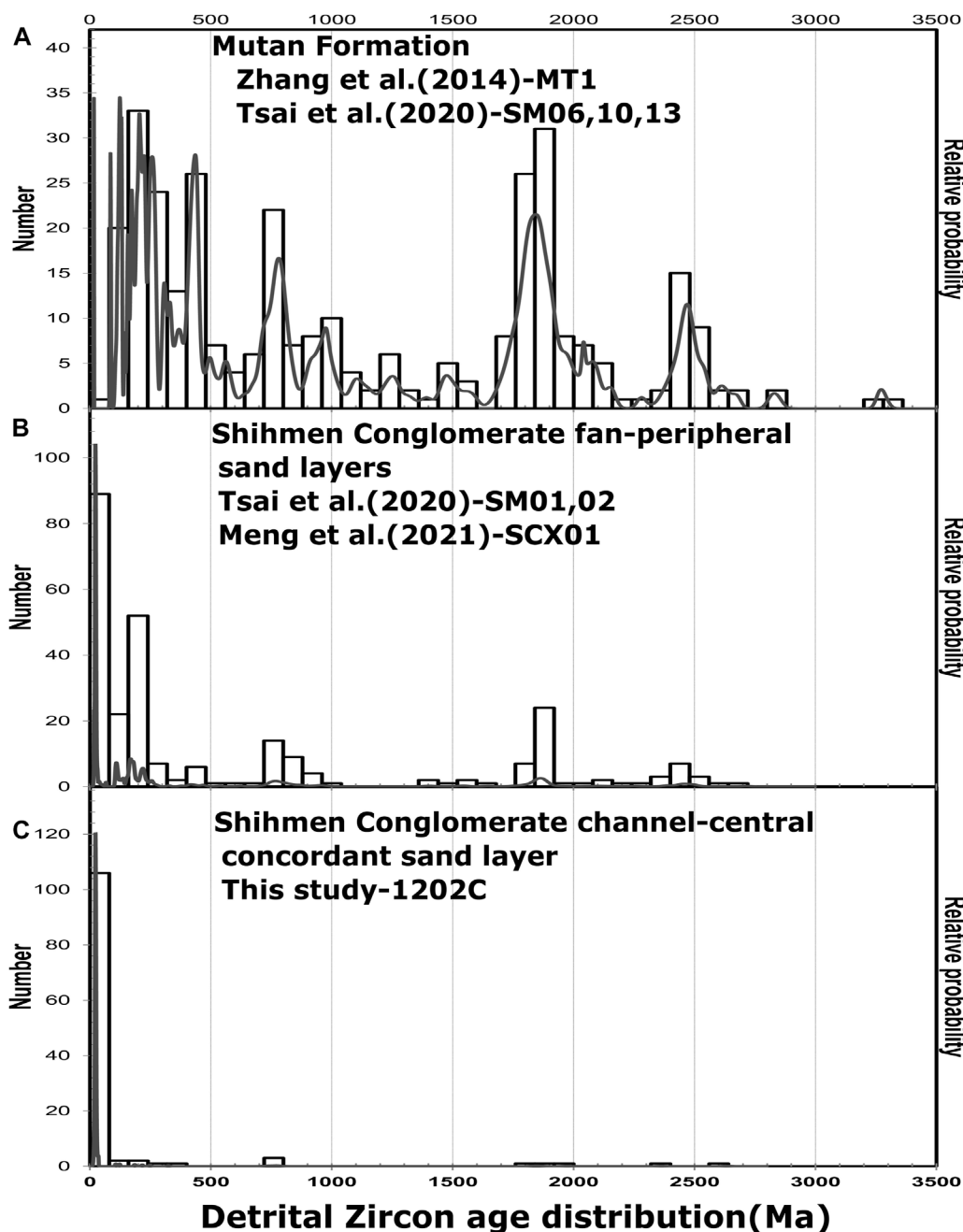


**FIGURE 6**  
 Detrital zircon age distribution diagrams for (A) common South China Sea turbidite sandstone of the Mutan Formation (Zhang et al., 2014; Tsai et al., 2020); (B) Turbidite sandstone adjacent to the Shihmen Conglomerate (Tsai et al., 2020; Meng et al., 2021); and (C) sandy layer within the Shihmen Conglomerate of sample 1202C.

The mechanism of the brief South China Sea obduction proposed above can be elucidated by the temporal relationships with tectonic events in the Manila subduction system and the Taiwan collisional orogeny. Immediately after seafloor spreading, the South China Sea was subducted under the Philippine Sea Plate along the Manila Trench since at least 15 Ma, as evidenced by the earliest arc magmatism (Lai et al., 2018; Figure 7A). The first continental subduction at the Manila Trench, which probably took place near present-day northern Taiwan due to the oblique

configuration between the trench and the COT (Suppe, 1988; Figure 7B), was estimated to be around 13 Ma (Chen et al., 2019) and was likely 11–9 Ma in central Taiwan, as inferred from the onset of blueschist retrograde cooling (Lo and Yui, 1996; Lo et al., 2020). The date of the obduction in question was close to these estimates of the initial impingement of the continent on the Manila Trench, which would induce major changes in the mechanical boundary conditions of the plate boundary (Malavieille and Trullenque, 2009) to cause the

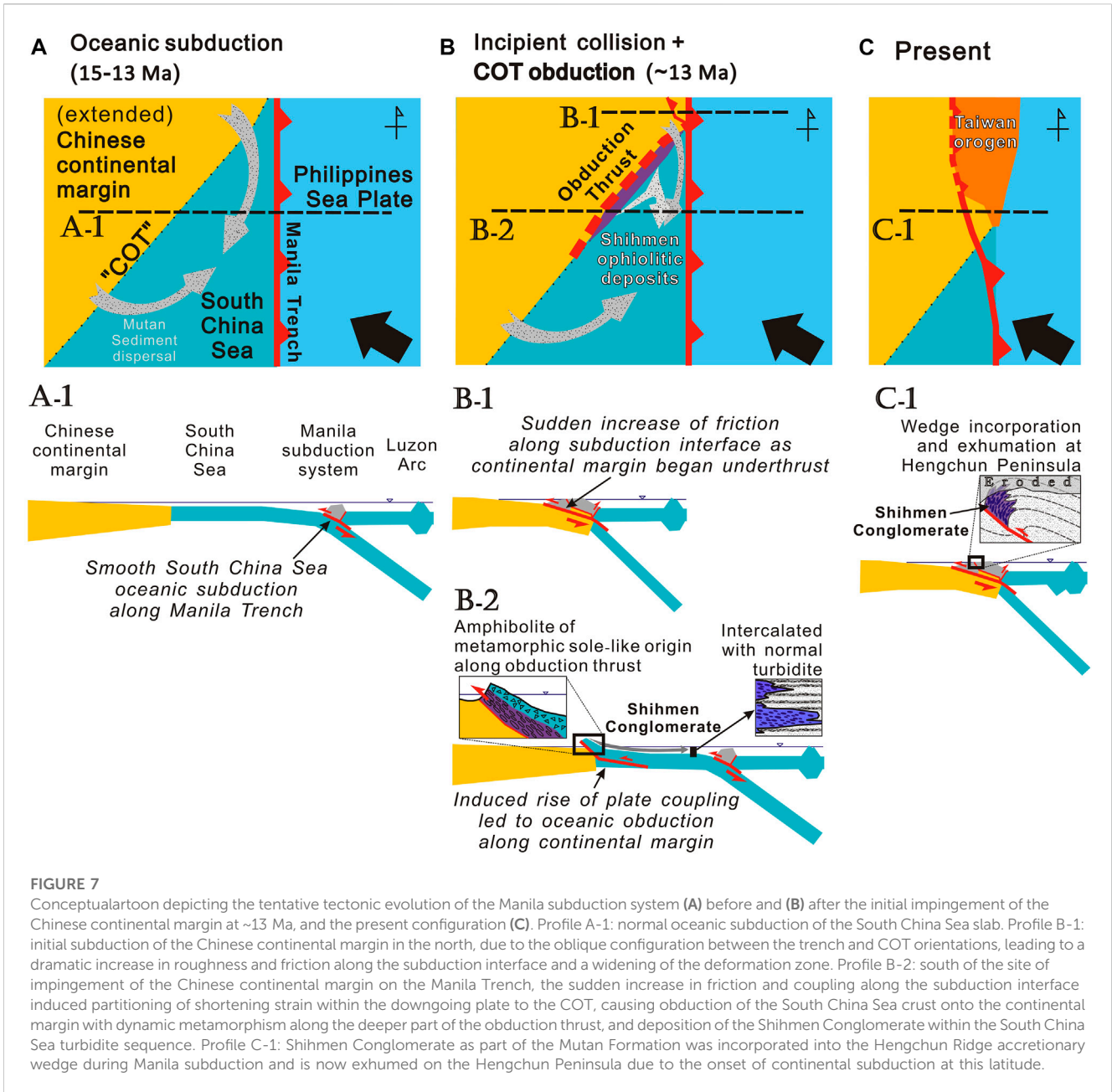


**FIGURE 7**

Conceptual cartoon depicting the tentative tectonic evolution of the Manila subduction system (A) before and (B) after the initial impingement of the Chinese continental margin at ~13 Ma, and the present configuration (C). Profile A-1: normal oceanic subduction of the South China Sea slab. Profile B-1: initial subduction of the Chinese continental margin in the north, due to the oblique configuration between the trench and COT orientations, leading to a dramatic increase in roughness and friction along the subduction interface and a widening of the deformation zone. Profile B-2: south of the site of impingement of the Chinese continental margin on the Manila Trench, the sudden increase in friction and coupling along the subduction interface induced partitioning of shortening strain within the downgoing plate to the COT, causing obduction of the South China Sea crust onto the continental margin with dynamic metamorphism along the deeper part of the obduction thrust, and deposition of the Shihmen Conglomerate within the South China Sea turbidite sequence. Profile C-1: Shihmen Conglomerate as part of the Mutan Formation was incorporated into the Hengchun Ridge accretionary wedge during Manila subduction and is now exhumed on the Hengchun Peninsula due to the onset of continental subduction at this latitude.

trench jump as the convergent strain was partitioned away from the trench itself (Chang et al., 2009b). Such mechanical transformation lies in the different frictional properties and seismic coupling of the subduction zone and is controlled by the roughness of the incoming seafloor (Lallemand et al., 2018), particularly the presence of cover-basement irregularities such as seamounts (Tan et al., 2022). Greater roughness is expected for the incorporation of continental crust with rugged topography and the cover-basement interface of the continental margin, causing strain partitioning from the subduction interface to a larger area, eventually leading to mountain building (Chang et al., 2009b; Malavieille et al., 2021). For an obliquely subducting oceanic slab such as the South China Sea, the initial arrival of the Eurasian continental margin at the Manila Trench in the north

would locally increase plate coupling and interface friction (profile B-1 of Figure 7B); a sudden interruption of subduction would divert a portion of the plate convergence to the COT southwestward as one of the major structural weaknesses within the descending plate, resulting in the simultaneous obduction of the South China Sea onto the Eurasian continental margin (Figure 7B). The hypothesized obduction would be short-lived, as the strain reorganization described above is transient in nature; therefore, the Shihmen Conglomerate has a rather limited temporal occurrence, no later than ~11 Ma. The Shihmen Conglomerate, as part of the South China Sea sedimentary succession (the Mutan Formation), was then incorporated into the accretionary wedge of the Manila subduction system and is now exhumed on the Hengchun Peninsula (Figure 7C).

## 5 Concluding remarks

The active arc-continent collision of the Taiwan mountain belt provides valuable insights into the evolution and growth of the East Asian continent, particularly the transition from oceanic to continental subduction. Due to oblique convergence, southernmost Taiwan is the youngest in orogenic history to record such a transition in both structures and stratigraphy. For the mafic-dominated Shihmen Conglomerate within the uplifted South China Sea turbidite sequence outcropping on the Hengchun Peninsula, new geochronological constraints indicate that a piece of early Miocene South China Sea crust dynamically metamorphosed at ~13 Ma, forming an isolated high-relief subaerial mountain range along the Chinese continental margin. This ephemeral mountain building of ophiolitic materials is best explained by an obduction event due to stress-strain reorganization of the Manila Trench during initial continental subduction. Such dramatic yet transient phenomena reveal the hidden tectonic complications in oceanic-continental subduction transitions, with important implications for the geodynamic evolution of continental margins.

## Data availability statement

The original contributions presented in the study are included in the article/[Supplementary Material](#), further inquiries can be directed to the corresponding author.

## Author contributions

Y-CL: field investigation, sample preparation, experiment, data analysis, scientific discussion, manuscript writing. C-TC: conceptualization, project planning, field investigation, data curation, scientific discussion, manuscript writing, funding acquisition. C-HL: conceptualization, project planning, data curation, scientific discussion, manuscript writing, funding acquisition. S-LC: experiment, data curation, scientific discussion. M-WY: experiment, data curation, scientific discussion.

## References

- Andersen, T. (2002). Correction of common lead in U-Pb analyses that do not report <sup>204</sup>Pb. *Chem. Geol.* 192, 59–79. doi:10.1016/s0009-2541(02)00195-x
- Beyssac, O., Simoes, M., Avouac, J.-P., Farley, K. A., Chen, Y. G., Chan, Y. C., et al. (2007). Late Cenozoic metamorphic evolution and exhumation of Taiwan. *Tectonics* 26, TC6001. doi:10.1029/2006tc002064
- Briaux, A., Patriat, P., and Tapponnier, P. (1993). Updated interpretation of magnetic anomalies and seafloor spreading stages in the south China sea: Implications for the tertiary tectonics of southeast asia/floor spreading stages in the South China sea: Implications for the tertiary tectonics of southeast asia. *J. Geophys. Res.* 98, 6299–6328. doi:10.1029/92jb02280
- Byrne, T., Chan, Y.-C., Rau, R.-J., Lu, C.-Y., Lee, Y.-H., and Wang, Y.-J. (2011). “The arc-continent collision in Taiwan,” in *Arc-continent collision: The making of an orogen*, *Frontiers in earth sciences*. Editors D. Brown and P. Ryan (Heidelberg: Springer), 211–243.
- Chang, C.-P., Angelier, J., and Huang, C.-Y. (2009b). “Evolution of subduction indicated by melanges in Taiwan,” in *Subduction zone geodynamics*. Editors S. Lallemand and F. Funiciello (Berlin: Springer), 207–225.
- Chang, C.-P., Angelier, J., Lee, T.-Q., and Huang, C.-Y. (2003). From continental margin extension to collision orogen: Structural development and tectonic rotation of the Hengchun peninsula, southern Taiwan. *Tectonophysics* 361, 61–82. doi:10.1016/s0040-1951(02)00561-9
- Chang, C.-P., Angelier, J., and Lu, C.-Y. (2009a). Polyphase deformation in a newly emerged accretionary prism: Folding, faulting and rotation in the southern Taiwan mountain range. *Tectonophysics* 466, 395–408. doi:10.1016/j.tecto.2007.11.002
- Chang, L.-S. (1964). A biostratigraphic study of the tertiary in the Hengchun Peninsula, Taiwan, based on smaller foraminifera (I: Northern Part). *Proceeding Geol. Soc. China* 7, 48–62.
- Chen, C.-H., Chu, H.-T., Liou, J. G., and Ernst, W. G. (1983). *Explanatory notes for the metamorphic facies map of Taiwan*. Taiwan: Special Publication of Central Geological Survey, 1–3.
- Chen, W.-S., Cheng, Y.-M., and Huang, C.-Y. (1985). Geology of the Hengchun peninsula, southern taiwan. *Ti-Chih* 6, 47–74.
- Chen, W.-S., Yeh, J.-J., and Syu, S.-J. (2019). Late Cenozoic exhumation and erosion of the Taiwan orogenic belt: New insights from petrographic analysis of foreland basin sediments and thermochronological dating on the metamorphic orogenic wedge. *Tectonophysics* 750, 56–69. doi:10.1016/j.tecto.2018.09.003

## Funding

This work was financially supported by grants from the National Science and Technology Council, Taiwan, R.O.C. to C-HL (111-2116-M-002-043- and 110-2116-M-002-029-) and C-TC (111-2116-M-008-019- and 108-2628-M-008-002-MY2).

## Acknowledgments

The authors are indebted to Hao-Tsu Chu for their invaluable knowledge and guidance on Hengchun geology and Taiwan tectonics.

## Conflict of interest

The authors declare that the research was conducted in the absence of any commercial or financial relationships that could be construed as a potential conflict of interest.

The handling editor MP declared a shared affiliation with the author SLC at the time of review.

## Publisher's note

All claims expressed in this article are solely those of the authors and do not necessarily represent those of their affiliated organizations, or those of the publisher, the editors and the reviewers. Any product that may be evaluated in this article, or claim that may be made by its manufacturer, is not guaranteed or endorsed by the publisher.

## Supplementary material

The Supplementary Material for this article can be found online at: <https://www.frontiersin.org/articles/10.3389/feart.2023.1118520/full#supplementary-material>

- Chi, W.-R. (1982). The calcareous nannofossils of the Lichi Melange and the Kenting Melange, and their significance in the interpretation of plate tectonics of the Taiwan region. *Ti-Chih* 4, 99–112.
- Chiu, H.-Y., Chung, S.-L., Wu, F.-Y., Liu, D., Liang, Y.-H., Lin, I.-J., et al. (2009). Zircon U-Pb and Hf isotopic constraints from eastern Transhimalayan batholiths on the precollisional magmatic and tectonic evolution in southern Tibet. *Tectonophysics* 477, 3–19. doi:10.1016/j.tecto.2009.02.034
- Chung, S.-L., and Sun, S.-S. (1992). A new genetic model for the East Taiwan ophiolite and its implications for dupal domains in the northern hemisphere. *Earth Planet. Sci. Lett.* 109, 133–145. doi:10.1016/0012-821x(92)90079-b
- Cui, Y., Shao, L., Yu, M., and Huang, C. (2021). Formation of Hengchun accretionary prism turbidites and implications for deep-water transport processes in the northern South China sea. *Acta Geol. Sin.* 95, 55–65. doi:10.1111/1755-6724.14640
- Denne, R. A. (2017). “Biostratigraphy,” in *Encyclopedia of petroleum geoscience. Encyclopedia of earth sciences series*. Editor R. Sorkhabi (Heidelberg: Springer), 20.
- Deschamps, A., Monié, P., Lallemand, S., Hsu, S. K., and Yeh, K. Y. (2000). Evidence for early cretaceous oceanic crust trapped in the Philippine Sea plate. *Earth Planet. Sci. Lett.* 179, 503–516. doi:10.1016/s0012-821x(00)00136-9
- Frost, B. R., and Frost, C. D. (2014). *Essentials of igneous and metamorphic petrology*. New York, USA: Cambridge University Press, 303.
- Gehrels, G. E., Valencia, V. A., and Ruiz, J. (2008). Enhanced precision, accuracy, efficiency, and spatial resolution of U-Pb ages by laser ablation-multicollector-inductively coupled plasma –mass spectrometry. *Geochem. Geophys. Geosystems* 9, Q03017. doi:10.1029/2007gc001805
- Harrison, T. M. (1982). Diffusion of <sup>40</sup>Ar in hornblende. *Contributions Mineralogy Petrology* 78, 324–331. doi:10.1007/bf00398927
- Hartmann, L. A., and Santos, J. O. S. (2004). Predominance of high Th/U, magmatic zircon in Brazilian Shield sandstones. *Geology* 32, 73–76. doi:10.1130/g20007.1
- Hoskin, P. W. O., and Black, L. P. (2000). Metamorphic zircon formation by solid-state recrystallization of protolith igneous zircon. *J. Metamorph. Geol.* 18, 423–439. doi:10.1046/j.1525-1314.2000.00266.x
- Hu, H.-N., and Tsan, S.-F. (1984). *Structural study of the slate formation along the South link railroad, taiwan*. Taiwan: Special Publication of Central Geological Survey, 25–43.
- Jackson, S. E., Pearson, N. J., Griffin, W. L., and Belousova, E. (2004). The application of laser ablation inductively coupled plasma mass spectrometry to *in-situ* U-Pb zircon geochronology. *Chem. Geol.* 211, 47–69. doi:10.1016/j.chemgeo.2004.06.017
- Jahn, B.-M., Wu, F., and Chen, B. (2000). Granitoids of the central asian orogenic belt and continental growth in the phanerozoic. *Trans. R. Soc. Edinb. Earth Sci.* 91, 181–193. doi:10.1017/s0263593300007367
- Karig, D. E., Ingle, J. C., Bouma, A. H., Ellis, C. H., Haile, N., Koizumi, I., et al. (1975). *Nitil reports of the deep sea drilling project*. in I. Washington, D.C.: U.S. Government Printing Office, 972.
- Koppers, A. A. P. (2002). ArArCALC-software for <sup>40</sup>Ar/<sup>39</sup>Ar age calculations. *Comput. Geosci.* 28, 605–619. doi:10.1016/s0098-3004(01)00095-4
- Lai, Y.-M., Chu, M.-F., Chen, W.-S., Shao, W.-Y., Lee, H.-Y., and Chung, S.-L. (2018). Zircon U-Pb and Hf isotopic constraints on the magmatic evolution of the Northern Luzon Arc. *Terr. Atmos. Ocean. Sci.* 29, 149–186. doi:10.3319/tao.2017.08.29.01
- Lallemand, S., Peyret, M., van Rijsingen, E., Arcay, D., and Heuret, A. (2018). Roughness characteristics of oceanic seafloor prior to subduction in relation to the seismogenic potential of subduction zones. *Geochem. Geophys. Geosystems* 19, 2121–2146. doi:10.1029/2018gc007434
- Lee, J. Y., Marti, K., Sevinghaus, J. P., Kawamura, K., Yoo, H. S., Lee, J. B., et al. (2006). A redetermination of the isotopic abundances of atmospheric Ar. *Geochimica Cosmochimica Acta* 70, 4507–4512. doi:10.1016/j.gca.2006.06.1563
- Lin, A. T., Yao, B., Hsu, S. K., Liu, C. S., and Huang, C. Y. (2009). Tectonic features of the incipient arc-continent collision zone of Taiwan: Implications for seismicity. *Tectonophysics* 479, 28–42. doi:10.1016/j.tecto.2008.11.004
- Lo, C. H., Chung, S. L., Lee, T. Y., and Wu, G. Y. (2002). Age of the Emeishan flood magmatism and relations to Permian-Triassic boundary events. *Earth Planet. Sci. Lett.* 198, 449–458. doi:10.1016/s0012-821x(02)00535-6
- Lo, C. H., and Yui, T. F. (1996). <sup>40</sup>Ar/<sup>39</sup>Ar dating of high-pressure rocks in the Tananao basement complex, Taiwan. *J. Geol. Soc. China* 39, 13–30.
- Lo, Y. C., Chen, C. T., Lo, C. H., and Chung, S. L. (2020). Ages of ophiolitic rocks along plate suture in Taiwan orogen: Fate of the South China Sea from subduction to collision. *Terr. Atmos. Ocean. Sci.* 31, 383–402. doi:10.3319/tao.2019.06.19.01
- Lu, C.-Y., and Hsu, K. J. (1992). Tectonic evolution of the Taiwan mountain belt. *Pet. Geol. Taiwan* 27, 21–46.
- Ludwig, K. R. (2008). *User's manual for isoplot/ex: A geochronological toolkit for microsoft excel*. Canterbury: Department of Computer Science University of Canterbury, 206–207.
- Malavieille, J., Dominguez, S., Lu, C. Y., Chen, C. T., and Konstantinovskaya, E. (2021). Deformation partitioning in mountain belts: Insights from analogue modelling experiments and the taiwan collisional orogen. *Geol. Mag.* 158, 84–103. doi:10.1017/s0016756819000645
- Malavieille, J., Lallemand, S. E., Domínguez, S., Deschamps, A., Lu, C. Y., Liu, C. S., et al. (2002). “Arc-continent collision in Taiwan: New marine observation and tectonic evolution,” in *Geology and geophysics of an Arc-Continent collision* (USA: Geological Society of America Special Paper), 189–213.
- Malavieille, J., and Trullenque, G. (2009). Consequences of continental subduction on forearc basin and accretionary wedge deformation in SE Taiwan: Insights from analogue modeling. *Tectonophysics* 466, 377–394. doi:10.1016/j.tecto.2007.11.016
- Meng, X., Shao, L., Cui, Y., Zhu, W., Qiao, P., Sun, Z., et al. (2021). Sedimentary records from Hengchun accretionary prism turbidites on Taiwan Island: Implication on late Neogene migration rate of the Luzon subduction system. *Mar. Petroleum Geol.* 124, 104820. doi:10.1016/j.marpetgeo.2020.104820
- Page, B. M., and Lan, C. Y. (1983). *The Kenting Mélange and its record of tectonic events*. China: Memoir of Geological Society of China, 227–248.
- Pelletier, B., and Stephan, J. F. (1986). Middle Miocene deduction and late Miocene beginning of collision registered in the Hengchun Peninsula: Geodynamic implications for the evolution of Taiwan. *Tectonophysics* 125, 133–160. doi:10.1016/0040-1951(86)90011-9
- Queano, K. L., Ali, J. R., Milsom, J., Aitchison, J. C., and Pubellier, M. (2007). North Luzon and the Philippine Sea Plate motion model: Insights following paleomagnetic, structural, and age-dating investigations. *J. Geophys. Res.* 112, B05101. doi:10.1029/2006jb004506
- Ryan, P. D., and Dewey, J. F. (2019). The Ordovician Grampian Orogeny, western Ireland: Obduction versus “bulldozing” during arc-continent collision. *Tectonics* 38, 3462–3475. doi:10.1029/2019TC005602
- Searle, M., Rioux, M., and Garber, J. M. (2022). One line on the map: A review of the geological history of the semai thrust, Oman-uae mountains. *J. Struct. Geol.* 158, 104594. doi:10.1016/j.jsg.2022.104594
- Sengor, A. M. C., Natal'in, B. A., and Burtman, V. S. (1993). Evolution of the Altai tectonic collage and Palaeozoic crustal growth in Eurasia. *Nature* 346, 299–307. doi:10.1038/364299a0
- Shyu, J. B. H., Sieh, K., and Chen, Y. G. (2005). Tandem suturing and disarticulation of the Taiwan orogen revealed by its neotectonic elements. *Earth Planet. Sci. Lett.* 233, 167–177. doi:10.1016/j.epsl.2005.01.018
- Sibuet, J. C., Hsu, S.-K., Le Pichon, X., Le Formal, J. P., Reed, D., Moore, G., et al. (2002). East asia plate tectonics since 15 Ma: Constraints from the taiwan region. *Tectonophysics* 344, 103–134. doi:10.1016/s0040-1951(01)00202-5
- Sláma, J., Košler, J., Condon, D. J., Crowley, J. L., Gerdes, A., Hanchar, J. M., et al. (2008). Plešovice zircon — a new natural reference material for U-Pb and Hf isotopic microanalysis. *Chem. Geol.* 249, 1–35. doi:10.1016/j.chemgeo.2007.11.005
- Song, S. R., and Lo, H. J. (2002). Lithofacies of volcanic rocks in the central Coastal Range, eastern Taiwan: Implications for island arc evolution. *J. Asian Earth Sci.* 21, 23–38. doi:10.1016/s1367-9120(02)00003-2
- Spell, T. L., and McDougall, I. (2003). Characterization and calibration of <sup>40</sup>Ar/<sup>39</sup>Ar dating standards. *Chem. Geol.* 198, 189–211. doi:10.1016/s0009-2541(03)00005-6
- Spencer, C. J., Kirkland, C. L., and Taylor, R. J. M. (2016). Strategies towards statistically robust interpretations of *in situ* U-Pb zircon geochronology. *Geosci. Front.* 7, 581–589. doi:10.1016/j.gsf.2015.11.006
- Sung, Q. (1991). Geologic map and the explanatory text for the Hengchun peninsula, geologic map of taiwan. *Scale* 1, 50000.
- Suppe, J. (1988). Tectonics of arc-continent collision on both sides of the South China sea: Taiwan and mindoro. *Acta Geol. Taiwanica* 26, 1–18.
- Tan, H., Gao, X., Wang, K., Gao, J., and He, J. (2022). Hidden roughness of subducting seafloor and implications for megathrust seismogenesis: Example from northern Manila Trench. *Geophys. Res. Lett.* 49, e2022GL100146. doi:10.1029/2022gl100146
- Taylor, B., and Hayes, D. E. (1983). “Origin and history of the South China Sea basin,” in *The tectonic and geologic evolution of southeast asian seas and islands: Part 2*. Editor D. E. Hayes (China: Geophysical Monograph Series), 23–56.
- Teng, L. S. (1990). Geotectonic evolution of late Cenozoic arc-continent collision in Taiwan. *Tectonophysics* 183, 57–76. doi:10.1016/0040-1951(90)90188-e
- Tian, Z. X., Yan, Y., Huang, C. Y., Zhang, X. C., Liu, H. Q., Yu, M. M., et al. (2019). Geochemistry and geochronology of the accreted mafic rocks from the Hengchun peninsula, southern taiwan: Origin and tectonic implications: crabs from the Hengchun peninsula, southern taiwan: Origin and tectonic implications. *J. Geophys. Res. Solid Earth* 124, 2469–2491. doi:10.1029/2018jb016562
- Tsai, C. H., Shyu, J. B. H., Chung, S.-L., and Lee, H. Y. (2020). Miocene sedimentary provenance and paleogeography of the Hengchun Peninsula, southern Taiwan: Implications for tectonic development of the Taiwan orogen. *J. Asian Earth Sci.* 194, 104032. doi:10.1016/j.jseas.2019.104032

- Vavra, G., Gebauer, D., Schmidt, R., and Compston, W. (1996). Multiple zircon growth and recrystallization during polyphase Late Carboniferous to Triassic metamorphism in granulites of the Ivrea Zone (southern Alps): An ion microprobe (SHRIMP) study. *Contributions Mineralogy Petrology* 122, 337–358. doi:10.1007/s004100050132
- Vermeesch, P. (2018). IsoplotR: A free and open toolbox for geochronology. *Geosci. Front.* 9, 1479–1493. doi:10.1016/j.gsf.2018.04.001
- Wang, K. L., Lo, Y. M., Chung, S. L., Lo, C. H., Hsu, S. K., Yang, H. J., et al. (2012). Age and geochemical features of dredged basalts from offshore SW Taiwan: The coincidence of intra-plate magmatism with the spreading South China Sea. *Terr. Atmos. Ocean. Sci.* 23, 657–669. doi:10.3319/tao.2012.07.06.01(tt)
- Wiedenbeck, M., Alle, P., Corfu, F., Grin, W. L., Meier, M., Oberli, F., et al. (1995). Three natural zircon standards for U-Th-Pb, Lu-Hf, trace element and REE analyses. *Geostand. Newsl.* 19, 1–23. doi:10.1111/j.1751-908x.1995.tb00147.x
- Williams, I. S., and Claesson, S. (1987). Isotopic evidence for the Precambrian provenance and Caledonian metamorphism of high grade paragneisses from the Sveve Nappes, Scandinavian Caledonides. II Ion microprobe zircon U-Th-Pb. *Contributions Mineralogy Petrology* 97, 205–217. doi:10.1007/bf00371240
- Yeh, Y. C., Sibuet, J. C., Hsu, S. K., and Liu, C. S. (2010). Tectonic evolution of the northeastern south China sea from seismic interpretation. *J. Geophys. Res.* 115, B06103. doi:10.1029/2009JB006354
- Zhang, X., Cawood, P. A., Huang, C. Y., Wang, Y., Yan, Y., Santosh, M., et al. (2016). From convergent plate margin to arc-continent collision: Formation of the Kenting Melange, Southern Taiwan. *Gondwana Res.* 38, 171–182. doi:10.1016/j.gr.2015.11.010
- Zhang, X., Yan, Y., Dilek, Y., Chen, W. H., and Shan, Y. (2022). Mid-Miocene uplift and tectonic-sedimentary evolution of the Taiwan accretionary prism: Constraints from sedimentary records in the Hengchun Peninsula, southern Taiwan. *Mar. Petroleum Geol.* 147, 105994. doi:10.1016/j.marpetgeo.2022.105994
- Zhang, X., Yan, Y., Huang, C. Y., Chen, D., Shan, Y., Lan, Q., et al. (2014). Provenance analysis of the Miocene accretionary prism of the Hengchun Peninsula, southern Taiwan, and regional geological significance. *J. Asian Earth Sci.* 85, 26–39. doi:10.1016/j.jseas.2014.01.021